

See discussions, stats, and author profiles for this publication at: <https://www.researchgate.net/publication/6343407>

# Interactions between Important Regulatory Proteins and Human $\alpha$ B Crystallin †

ARTICLE *in* BIOCHEMISTRY · JUNE 2007

Impact Factor: 3.02 · DOI: 10.1021/bi700149h · Source: PubMed

---

CITATIONS

60

---

READS

48

3 AUTHORS, INCLUDING:



[John I Clark](#)

University of Washington Seattle

**159** PUBLICATIONS **4,691** CITATIONS

SEE PROFILE

Interactions between Important Regulatory Proteins and Human  $\alpha$ B Crystallin<sup>†</sup>Joy G. Ghosh,<sup>‡,§,||</sup> Ananth K. Shenoy, Jr.,<sup>§,||</sup> and John I. Clark<sup>\*,‡,§,⊥</sup>*Biomolecular Structure and Design, Department of Biological Structure, and Department of Ophthalmology, University of Washington, Seattle, Washington 98195-7420**Received January 24, 2007; Revised Manuscript Received March 21, 2007*

**ABSTRACT:** Protein pin arrays assessed interactions between  $\alpha$ B crystallin and 12 regulatory proteins, including EGF, FGF-2, IGF-1, NGF- $\beta$ , TGF- $\beta$ , VEGF, insulin,  $\beta$ -catenin, caspase-3, caspase-8, Bcl-2, and Bcl-x<sub>L</sub>, which are important in cellular differentiation, proliferation, signaling, cytoskeletal assembly, and apoptosis. FGF-2, NGF- $\beta$ , VEGF, insulin, and  $\beta$ -catenin had strong interactions with human  $\alpha$ B crystallin peptides, and the  $\alpha$ B crystallin interactive sequences for these proteins were identified. The seven remaining proteins (EGF, IGF-1, TGF- $\beta$ , caspase-3, caspase-8, Bcl-2, and Bcl-x<sub>L</sub>) did not interact with  $\alpha$ B crystallin. The  $\alpha$ B crystallin sequences that interacted with FGF-2, NGF- $\beta$ , VEGF, insulin, and  $\beta$ -catenin overlapped with sequences that selectively interact with partially unfolded proteins, suggesting a common function for  $\alpha$ B crystallin in chaperone activity and the regulation of cell growth and differentiation. Chaperone assays conducted with full-length  $\alpha$ B crystallin and synthetic  $\alpha$ B crystallin peptides confirmed the ability of  $\alpha$ B crystallin to protect against the aggregation of FGF-2 and VEGF, suggesting that  $\alpha$ B crystallin protects these proteins against unfolding and aggregation under conditions of stress. This is the first report in which sequences involved in interactions with regulatory proteins, including FGF-2, NGF- $\beta$ , VEGF, insulin, and  $\beta$ -catenin, were identified in a small heat shock protein.

Small heat shock proteins (sHSPs)<sup>1</sup> make up a class of molecular chaperones with molecular masses of <43 kDa that display a low degree of sequence similarity, contain a highly conserved immunoglobulin-like structural fold called the  $\alpha$  crystallin core domain, and are upregulated in response to cellular stress (1–5). Human  $\alpha$ B crystallin is the archetype for sHSPs and “unfolding response proteins” (URP) that respond to protein unfolding and misfolding under conditions of cellular stress (6, 7). The molecular chaperone activity of sHSPs, which involves the recognition, binding, solubility, and refolding of a wide range of structurally unrelated proteins in various states of unfolding, is considered their most prominent functional role in vivo (8–11). In addition to recognizing, binding, and stabilizing structurally compromised proteins during or after various forms of stress, sHSPs interact with growth factors and filaments under physiological conditions, suggesting a functional role for sHSPs in normal development (6, 9, 12–16). sHSPs play an important role in organizing and stabilizing cytoskeleton filament networks (8, 10, 14, 17–26). Mammalian sHSPs, including  $\alpha$ B crystallin, sHSP20, sHSP22, sHSP25/27, sHSPB2,

sHSPB3, cvHSP, sHSPB9, and  $\alpha$ A crystallin, are constitutively expressed during development and are believed to be important in cellular processes that include cell morphogenesis, inflammatory response, cell proliferation, mitogenesis, platelet function, and cell differentiation (9, 11, 27–37). The interactions between sHSPs and proteins involved in regulatory pathways have not been studied systematically, and surface domains that mediate these interactions in sHSPs have not been identified.

Under physiological conditions,  $\alpha$ B crystallin is a soluble cytosolic protein. Under conditions of stress or in pathologies like Alzheimer’s disease, Parkinson’s disease, and age-related macular degeneration (AMD) (38, 39),  $\alpha$ B crystallin migrates into the nucleus and colocalizes in extracellular plaques, in Lewy bodies, in Drusen, or with the plasma membrane (40–49).  $\alpha$ B crystallin localizes with  $\beta$ -catenin and other regulatory proteins involved in actin dynamics and cell adhesion at the leading edges of migrating lens epithelial cells (50). Cell migration is a dynamic process that involves rapid conformational changes in proteins that require protective chaperone-like activities to prevent aggregation. It is likely that  $\alpha$ B crystallin is a chaperone for  $\beta$ -catenin and other regulatory proteins involved in cell migration under conditions of mechanical stress and strain. FGF-2 lacks the classical signaling sequences required for ER–Golgi mediated secretion, and an alternate hypothesis for its extracellular secretion and trafficking may involve chaperone proteins (51).  $\alpha$ B crystallin associates with the Golgi apparatus (52, 53) and has a high affinity for phospholipid vesicles (47). An association with  $\alpha$ B crystallin may sequester FGF-2 molecules into phospholipid vesicles, enabling their transport and secretion, especially under conditions of stress. The presence of  $\alpha$ B crystallin in blood plasma and cerebrospinal

<sup>†</sup> Supported by Grant EY04542 from the National Eye Institute.

\* To whom correspondence should be addressed: Department of Biological Structure, HSB G514, Box 357420, University of Washington, Seattle, WA 98195-7420. E-mail: clarkji@u.washington.edu. Phone: (206) 685-0950. Fax: (206) 543-1524.

<sup>‡</sup> Biomolecular Structure and Design.

<sup>§</sup> Department of Biological Structure.

<sup>||</sup> These authors contributed equally to this work.

<sup>⊥</sup> Department of Ophthalmology.

<sup>1</sup> Abbreviations: sHSP, small heat shock protein; EGF, epidermal growth factor; FGF-2, fibroblast growth factor; IGF-1, insulin-like growth factor; NGF- $\beta$ , nerve growth factor; TGF- $\beta$ , transforming growth factor; VEGF, vascular endothelial growth factor; MOE, Molecular Operating Environment.

Table 1: Proteins and Antibodies Used in the Pin Array and Chaperone Assays

protein or peptide	catalog no.	supplier	molecular mass (kDa)	concentration ( $\mu$ M)
rhEGF	RDI-115	Research Diagnostics	6.2	0.2419
rhFGF-2	234-FSE	R&D Systems	17.4	0.0052
rhFGF-2	00081101	National Cancer Institute	16	3.12
rhIGF-1	RDI-111	Research Diagnostics	7.6	0.1974
rhNGF- $\beta$	N 1408	Sigma	27	0.0185
rhTGF-1 $\beta$	89091902	National Cancer Institute	25	0.0003
rhVEGF	32203	National Cancer Institute	34	0.2206
rh insulin	I-0259	Sigma	5.8	1.5497
rhBcl-2	827-BC	R&D Systems	27	0.0926
rhBcl-xL	894-BX	R&D Systems	28	0.0893
rhcaspase-3	707-C3/CF	R&D Systems	28	0.0179
rhcaspase-8	218769	Calbiochem	55	0.0005
rh $\beta$ -catenin	n/a <sup>a</sup>	Purified	86	0.0249
rh $\alpha$ B crystallin	n/a <sup>a</sup>	Purified	20.2	n/a <sup>a</sup>
DRFSVNLDVKHFS	custom synthesis	Advanced ChemTech	1.6	n/a <sup>a</sup>
LTITSSLSGDV	custom synthesis	GenScript Corp.	1.1	n/a <sup>a</sup>
FISREFHR	custom synthesis	GenScript Corp.	1.1	n/a <sup>a</sup>
ERTIPITRE	custom synthesis	GenScript Corp.	1.1	n/a <sup>a</sup>
antibody	catalog no.	supplier	primary Ab dilution	secondary Ab dilution
rabbit polyclonal anti-EGF	RDI-EGFabrP	Research Diagnostics	400	10000
mouse monoclonal anti-FGF- $\beta$	F6162	Sigma	40000	40000
rabbit polyclonal anti-IGF-1	RDI-ILGF1abrP	Research Diagnostics	400	20000
rabbit polyclonal anti-NGF- $\beta$	RDI-NGFabrP	Research Diagnostics	2000	10000
rabbit polyclonal anti-TGF- $\beta$	3711	Cell Signaling Technology	5000	40000
rabbit polyclonal anti-VEGF	RDI-VEGFabrP	Research Diagnostics	5000	20000
mouse monoclonal anti-insulin	I2018	Sigma	500	20000
mouse monoclonal anti-Bcl-2	MAB827	R&D Systems	2000	20000
mouse monoclonal anti-Bcl-xL	2300-MC	R&D Systems	5000	40000
mouse monoclonal anti-caspase-3	MAB707	R&D Systems	5000	40000
rabbit polyclonal anti-caspase-8	51-1100	Zymed	5000	40000
mouse monoclonal anti- $\beta$ -catenin	RDI-BCATENINabm	Research Diagnostics	250	20000
rabbit anti-mouse IgG-HRP	A 9044	Sigma	n/a <sup>a</sup>	n/a <sup>a</sup>
goat anti-rabbit IgG-HRP	SAB-300	Stressgen	n/a <sup>a</sup>	n/a <sup>a</sup>

<sup>a</sup> Not applicable.

fluid, and the increased level of expression of  $\alpha$ B crystallin after stroke and under neurological conditions, suggest that similar pathways may mediate the stabilization and secretion of VEGF, NGF- $\beta$ , and insulin (54, 55). The intracellular and extracellular physiological actions of  $\alpha$ B crystallin and the specific function of individual interactive sequences in the folding, stability, and function of signaling molecules like FGF, VEGF, and  $\beta$ -catenin are an important area for future studies of sHSPs in normal cell activities and in disease.

This study used protein pin arrays to identify interactive sequences in human  $\alpha$ B crystallin for selected proteins reported to be involved in the cellular pathways that are important for cell differentiation (12, 31, 37, 50, 56–61). Protein pin array analysis determined that human  $\alpha$ B crystallin contained interactive sequences for FGF-2, NGF- $\beta$ , VEGF, insulin, and  $\beta$ -catenin, while EGF, IGF-1, TGF- $\beta$ , Bcl-2, Bcl-xL, caspase-3, and caspase-8 had no interactions with  $\alpha$ B crystallin. The  $\alpha$ B crystallin sequences that had the strongest interactions with FGF-2, NGF- $\beta$ , VEGF, insulin, and  $\beta$ -catenin overlapped with previously identified  $\alpha$ B crystallin chaperone and filament interactive sequences, suggesting that  $\alpha$ B crystallin may be important for the folding and processing of these proteins in vivo. Chaperone assays conducted with full-length wt human  $\alpha$ B crystallin and synthesized  $\alpha$ B crystallin interactive sequences 73-DRFSVNLDVKHFS<sub>85</sub>, 113FISREFHR<sub>120</sub>, 131LTITSSLS-DGV<sub>141</sub>, and 156ERTIPITRE<sub>164</sub> confirmed that  $\alpha$ B crystallin protected FGF-2 and VEGF from unfolding and aggregation through its surface interactive sequences.

## EXPERIMENTAL PROCEDURES

**ELISA-Based Protein Pin Array Assay.** Proteins and antibodies used in the protein pin array assay are listed in Table 1. The protein pin array assays were performed as described previously with each protein being assayed two or three times (61). The loss of efficiency of the protein pin array was measured as described previously and was found to be insignificant for up to 30 assays (60, 61). For each target protein, the pin array quantifies differences in interactions between peptides on the pin array and the target protein (61). When a new target protein is used, the antibody reactions and affinities change so quantitative comparisons are difficult to make for different target proteins. Quantitative and systematic validation of the pin array results using SPR (62) and other binding assays are being conducted to compare binding between  $\alpha$ B crystallin and different target proteins.

**Chaperone Assays.** The effect of full-length  $\alpha$ B crystallin and synthetic  $\alpha$ B crystallin peptides on the thermal unfolding and aggregation of FGF-2 was measured as described previously (12). Briefly, 3.12  $\mu$ M FGF-2 was incubated in the absence and presence of 3.12  $\mu$ M full-length  $\alpha$ B crystallin or synthetic  $\alpha$ B crystallin peptides 73-DRFSVNLDVKHFS<sub>85</sub>, 113FISREFHR<sub>120</sub>, and 131LTITSSLSGDV<sub>142</sub> in 200  $\mu$ L of 10 mM PBS buffer (pH 7.2). The optical density at 360 nm (OD<sub>360</sub>) was measured at 10 min intervals for 90 min at 45 °C using a Pharmacia Biotech Ultrospec 3000 spectrophotometer. The OD<sub>360</sub> of FGF alone after 90 min was set to 100% aggregation. The effect of full-length  $\alpha$ B crystallin

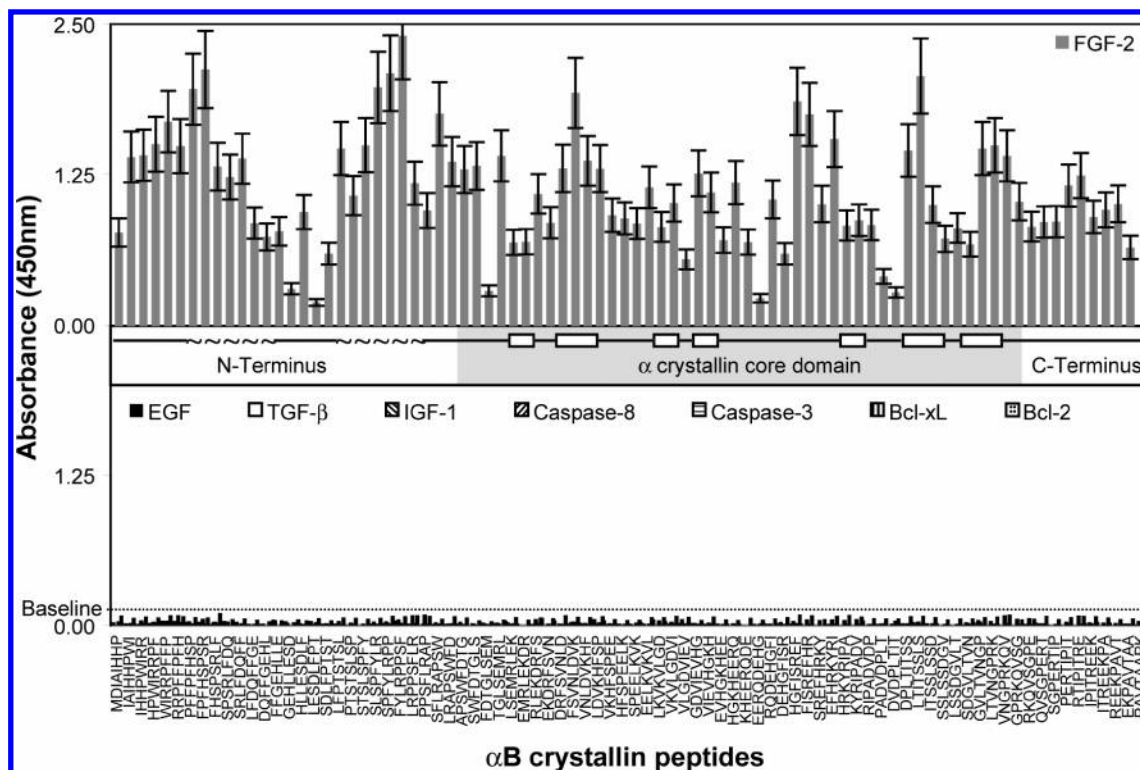


FIGURE 1: Interactions between  $\alpha$ B crystallin peptides and EGF, TGF- $\beta$ , IGF-1, caspase-3, caspase-8, Bcl-2, Bcl-x<sub>L</sub>, and FGF-2. The amino acid sequences of the overlapping  $\alpha$ B crystallin peptides are plotted on the X-axis. The absorbances of the  $\alpha$ B crystallin peptides in the presence of EGF (black bars), TGF- $\beta$  (white bars), IGF-1 (left diagonally striped bars), caspase-3 (horizontally striped bars), caspase-8 (right diagonally striped bars), Bcl-2 (dotted bars), Bcl-x<sub>L</sub> (vertically striped bars), and FGF-2 (gray bars) are plotted on the Y-axis. The predicted secondary structure of  $\alpha$ B crystallin based on homology modeling and electron spin resonance studies is shown in the plot (~ for helix and  $\square$  for  $\beta$  strand). The three structural domains of  $\alpha$ B crystallin, the N-terminal domain, the  $\alpha$  crystallin core domain, and the C-terminal domain, are shown below the secondary structure. In the presence of FGF-2, 83 of 84  $\alpha$ B crystallin peptides had absorbances higher than the baseline ( $Abs_{450} = 0.10$ ). In the presence of EGF, TGF- $\beta$ , IGF-1, caspase-3, caspase-8, Bcl-2, and Bcl-x<sub>L</sub>, none of the 84  $\alpha$ B crystallin peptides had absorbances higher than the baseline. FGF-2 interacts with  $\alpha$ B crystallin, while EGF, TGF- $\beta$ , IGF-1, caspase-3, caspase-8, Bcl-2, and Bcl-x<sub>L</sub> have no measurable interactions with  $\alpha$ B crystallin.

and synthetic  $\alpha$ B crystallin peptides on the dithiothreitol (DTT)-induced unfolding and aggregation of VEGF was measured as described below. VEGF (1.48  $\mu$ M) was incubated in the absence and presence of 1.48  $\mu$ M full-length  $\alpha$ B crystallin or synthetic  $\alpha$ B crystallin peptides  $_{113}$ FISREFHR $_{120}$  and  $_{156}$ ERTIPITRE $_{164}$  in 200  $\mu$ L of 10 mM PBS buffer (pH 7.2) and 75  $\mu$ M DTT. The optical density at 360 nm ( $OD_{360}$ ) was measured at 10 min intervals for 90 min at 37  $^{\circ}$ C using a Pharmacia Biotech Ultrospec 3000 spectrophotometer. The  $OD_{360}$  of the VEGF alone after 90 min was set to 100% aggregation.

The aggregation of FGF and VEGF in the presence of full-length  $\alpha$ B crystallin and the synthetic  $\alpha$ B crystallin peptides was assessed as a percentage of the aggregation of FGF or VEGF alone as follows:

$$\% \text{ aggregation} = \frac{OD_{360} (\text{VEGF/FGF} + \alpha\text{B crystallin peptide})}{OD_{360} (\text{VEGF/FGF alone})}$$

## RESULTS

Interactions between peptides of the  $\alpha$ B crystallin protein pin array and 12 proteins (EGF, IGF-1, TGF- $\beta$ , Bcl-2, Bcl-x<sub>L</sub>, caspase-3, caspase-8, FGF-2, NGF- $\beta$ , VEGF, insulin, and  $\beta$ -catenin) were assessed using a pin array assay. In the presence of human FGF-2 (Figure 1, gray bars), 83 of the 84  $\alpha$ B crystallin peptides had absorbances higher than the baseline ( $Abs_{450} = 0.10$ ), with the peptide  $_{47}$ FYLRPPSF $_{54}$

having the highest absorbance ( $Abs_{450} = 2.42$ ). These 83  $\alpha$ B crystallin peptides formed a pattern of five absorbance peaks where the maximum absorbance was recorded as a central peptide flanked by peptides with lower absorbances. The central peptides  $_{15}$ FPFHSPSR $_{22}$ ,  $_{47}$ FYLRPPSF $_{54}$ ,  $_{75}$ FSVNLDVK $_{82}$ ,  $_{111}$ HGFISREF $_{120}$ , and  $_{131}$ LTITSSLS $_{138}$  from each peak were identified as interactive peptides in  $\alpha$ B crystallin that mediated interactions with FGF-2. In contrast, when EGF, TGF- $\beta$ , Bcl-2, Bcl-x<sub>L</sub>, caspase-3, and caspase-8 were assayed for interactions with the  $\alpha$ B crystallin pin array, no absorbances higher than the baseline ( $Abs_{450} = 0.10$ ) were measured. The absence of absorbances higher than the baseline absorbance indicated that these proteins did not interact with the  $\alpha$ B crystallin peptides.

The absorbances of 64 of the 84  $\alpha$ B crystallin peptides were higher than the baseline ( $Abs_{450} = 0.10$ ) when NGF- $\beta$  was the ligand in the pin array assay (Figure 2, gray bars). The 64  $\alpha$ B crystallin peptides that interacted with NGF- $\beta$  formed a pattern of four absorbance maxima for peptides that had the highest absorbance flanked by peptides with lower absorbances. Absorbance maxima were recorded for the peptides  $_{53}$ SFLRAPSW $_{60}$ ,  $_{113}$ FISREFHR $_{120}$ ,  $_{131}$ LTITSSLS $_{138}$ , and  $_{143}$ LTVNGPRK $_{150}$ . These peptides were identified as NGF- $\beta$  interactive peptides in human  $\alpha$ B crystallin. All four interactive sequences were localized in the N-terminal domain and the  $\alpha$  crystallin core domain. When VEGF was the ligand in the pin array assay



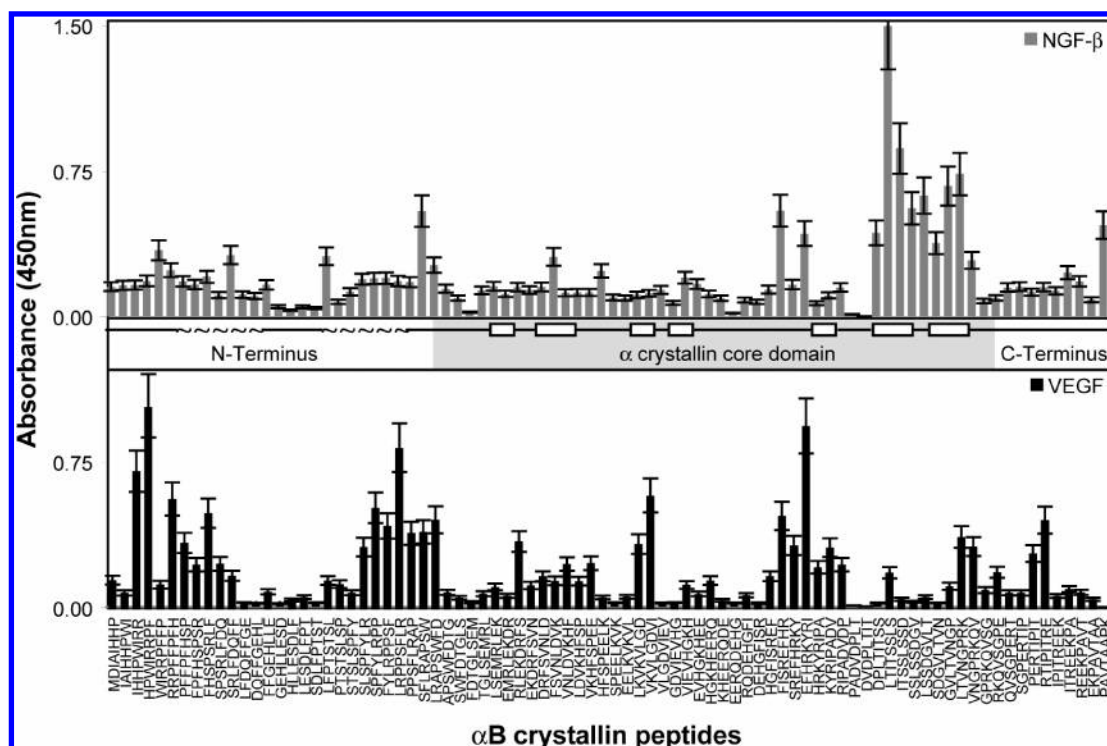


FIGURE 2: Interactions between  $\alpha$ B crystallin peptides and NGF- $\beta$  and VEGF. The amino acid sequences of the overlapping  $\alpha$ B crystallin peptides are plotted on the X-axis. The absorbances of the  $\alpha$ B crystallin peptides in the presence of NGF- $\beta$  (gray bars) and VEGF (black bars) are plotted on the Y-axis. The predicted secondary structure of  $\alpha$ B crystallin based on homology modeling and electron spin resonance studies is shown in the plot ( $\sim$  for helix and  $\square$  for  $\beta$  strand). The three structural domains of  $\alpha$ B crystallin, the N-terminal domain, the  $\alpha$  crystallin core domain, and the C-terminal domain, are shown below the secondary structure. In the presence of NGF- $\beta$ , 64 of 84  $\alpha$ B crystallin peptides had absorbances higher than the baseline ( $Abs_{450} = 0.10$ ), and in the presence of VEGF, 47 of 84  $\alpha$ B crystallin peptides had absorbances higher than the baseline.

(Figure 2, black bars), 47 of the 84  $\alpha$ B crystallin peptides had absorbances higher than the baseline, with the peptide  $\gamma$ HPWIRPF<sub>14</sub> having the highest absorbance ( $Abs_{450} = 1.04$ ). The 47  $\alpha$ B crystallin peptides that interacted with VEGF formed a pattern of six absorbance maxima for peptides that had the highest absorbance flanked by peptides with lower absorbances. Absorbance maxima were recorded for the peptides  $\gamma$ HPWIRPF<sub>14</sub>,  $^{49}$ LRPPSFLR<sub>56</sub>,  $^{91}$ VKV-LGDVI<sub>98</sub>,  $^{117}$ EFHRKYRI<sub>124</sub>,  $^{143}$ LTVNGPRK<sub>150</sub>, and  $^{157}$ RTIPITRE<sub>164</sub>, which were identified as VEGF interactive peptides in human  $\alpha$ B crystallin.

Similar to those of NGF- $\beta$  and VEGF, interactions between  $\alpha$ B crystallin peptides and two signaling molecules, human insulin (Figure 3, gray bars) and human  $\beta$ -catenin (Figure 3, black bars), were assessed using the pin array assay. When human insulin was the ligand in the pin array assay, all 84  $\alpha$ B crystallin peptides had absorbances higher than the baseline and the maximum absorbance ( $Abs_{450} = 1.25$ ) was recorded for the peptide  $^{165}$ EKPAVTAA<sub>172</sub>. A pattern of nine absorbance peaks was observed with maximum absorbances being recorded for the peptides  $^{11}$ -RRPFFPFH<sub>18</sub>,  $^{33}$ LESDFLPT<sub>40</sub>,  $^{49}$ LRPPSFLR<sub>56</sub>,  $^{75}$ FSVNLDVK<sub>82</sub>,  $^{93}$ VLGDVIEV<sub>100</sub>,  $^{125}$ PADVDP<sub>132</sub>,  $^{137}$ LSSDGVLT<sub>144</sub>,  $^{151}$ QVSGPERT<sub>158</sub>, and  $^{165}$ EKPAVTAA<sub>172</sub>, which were identified as insulin interactive peptides in human  $\alpha$ B crystallin. When human  $\beta$ -catenin was the ligand in the pin array assay, 76 of the 84  $\alpha$ B crystallin peptides had absorbances higher than the baseline ( $Abs_{450} = 0.10$ ), and the maximum absorbance ( $Abs_{450} = 0.79$ ) was recorded for the peptide  $^{47}$ -FYLRPPSF<sub>54</sub>. A pattern of seven absorbance peaks was observed with maximum absorbances being recorded for the

peptides  $^{13}$ PFFPFHSP<sub>20</sub>,  $^{47}$ FYLRPPSF<sub>54</sub>,  $^{75}$ FSVNLDVK<sub>82</sub>,  $^{89}$ -LKVVLGD<sub>96</sub>,  $^{113}$ FISREFHR<sub>120</sub>,  $^{131}$ LTITSSLS<sub>138</sub>, and  $^{145}$ -VNGPRKQV<sub>152</sub>, which were identified as  $\beta$ -catenin interactive peptides in human  $\alpha$ B crystallin.

The  $\alpha$ B crystallin sequences  $^{73}$ DRFSVNLDVKHFS<sub>85</sub>,  $^{113}$ -FISREFHR<sub>120</sub>, and  $^{131}$ LTITSSLS<sub>142</sub> that had strong interactions with FGF-2 were previously identified as chaperone sequences in human  $\alpha$ B crystallin. Consequently, these three peptides were synthesized and tested for their individual effect on the thermal aggregation of FGF-2 (Figure 4, gray bars). In the presence of full-length wt human  $\alpha$ B crystallin, the extent of thermal aggregation of FGF-2 was approximately 70% of the extent of aggregation in the absence of wt  $\alpha$ B crystallin. In the presence of the peptides DRFSVNLDVKHFS and LTITSSLS<sub>142</sub>, the level of aggregation of FGF-2 was 39 and 28%, respectively, a much stronger effect on aggregation than that for full-length wt  $\alpha$ B crystallin. In the presence of the FISREFHR peptide, the level of FGF-2 aggregation increased approximately 26%, although in the presence of a 10-fold excess of FISREFHR (31  $\mu$ M), the level of FGF-2 aggregation decreased to 42% (data not shown). Similarly, the ability of full-length human  $\alpha$ B crystallin and two synthetic  $\alpha$ B crystallin peptides,  $^{113}$ -FISREFHR<sub>120</sub> and  $^{156}$ ERTIPITRE<sub>164</sub>, to inhibit the DTT-induced aggregation of VEGF was assessed spectroscopically (Figure 4, black bars). Full-length wt human  $\alpha$ B crystallin decreased the level of VEGF aggregation by approximately 57%, while the FISREFHR and ERTIPITRE peptides decreased the level of VEGF aggregation by approximately 43%. Together, these results confirmed the importance of the interactive sequences in the  $\alpha$  crystallin core domain and

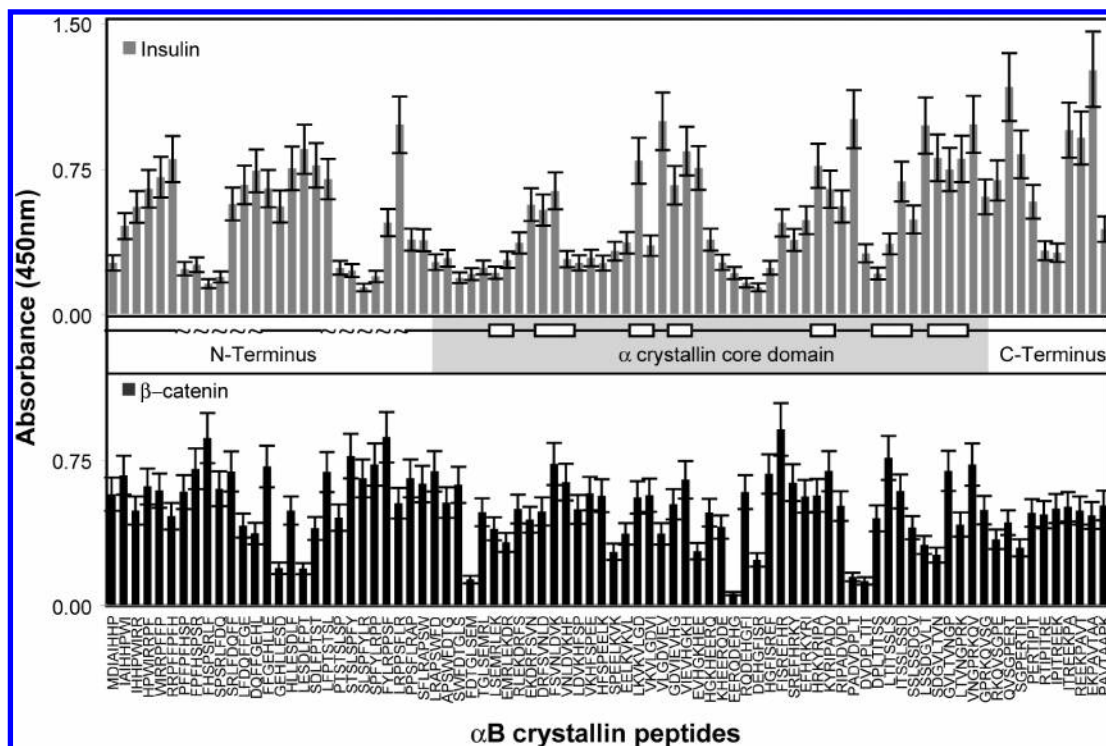


FIGURE 3: Interactions between  $\alpha$ B crystallin peptides and  $\beta$ -catenin and insulin. The amino acid sequences of the overlapping  $\alpha$ B crystallin peptides are plotted on the X-axis. The absorbances of the  $\alpha$ B crystallin peptides in the presence of insulin (gray bars) and  $\beta$ -catenin (black bars) are plotted on the Y-axis. The predicted secondary structure of  $\alpha$ B crystallin based on homology modeling and electron spin resonance studies is shown in the plot ( $\sim$  for helix and  $\square$  for  $\beta$  strand). The three structural domains of  $\alpha$ B crystallin, the N-terminal domain, the  $\alpha$  crystallin core domain, and the C-terminal domain, are shown below the secondary structure. In the presence of insulin, all 84  $\alpha$ B crystallin peptides had absorbances higher than the baseline ( $Abs_{450} = 0.10$ ), while in the presence of  $\beta$ -catenin, 76 of 84  $\alpha$ B crystallin peptides had absorbances higher than the baseline.

C-terminal extension for chaperone activity of  $\alpha$ B crystallin with the growth factors FGF-2 and VEGF.

The  $\alpha$ B crystallin interactive sequences for subunit–subunit interactions, chaperone activity, filament interactions, and interactions with growth factors, insulin, and  $\beta$ -catenin were compared for similarities in secondary structure and mapped to the surface of the three-dimensional model of human  $\alpha$ B crystallin (Figure 5). Overlap was observed in four regions of  $\alpha$ B crystallin, including the  $\beta$ 3,  $\beta$ 8, and  $\beta$ 9 sequences in the  $\alpha$  crystallin core domain, and the C-terminal extension containing the conserved Ile-X-Ile motif. The  $\beta$ 3,  $\beta$ 8, and  $\beta$ 9 sequences were localized in the same region of the  $\alpha$  crystallin core domain and formed a surface for interactions with various types of substrate proteins. Although  $\alpha$ B crystallin contains conserved surfaces that interact with a wide variety of proteins, there appear to be additional surfaces that are selective for interactions with specific protein targets. The collective response of these interactive surfaces results in the recognition, stabilization, solubility, and refolding of structurally compromised substrates by full-length  $\alpha$ B crystallin.

## DISCUSSION

Twelve proteins important for cell differentiation and development were evaluated in this study, and FGF-2, NGF- $\beta$ , VEGF, insulin, and  $\beta$ -catenin were determined to interact positively with specific sequences in human  $\alpha$ B crystallin. These results were consistent with previous reports in which  $\alpha$ B crystallin was shown to be involved in pathways involving FGF-2, NGF- $\beta$ , VEGF,  $\beta$ -catenin, and insulin (12,

31, 37, 50, 56–58).  $\alpha$ B crystallin sequences that had strong interactions with NGF- $\beta$ , VEGF, insulin,  $\beta$ -catenin, and FGF-2 overlapped with sequences that were previously identified as chaperone sequences in  $\alpha$ B crystallin (60, 63, 64) (Figure 5). The overlap between the interactive sequences for FGF-2, NGF- $\beta$ , VEGF, insulin, and  $\beta$ -catenin and the chaperone sequences of  $\alpha$ B crystallin suggested a functional relationship among key elements of signaling pathways for cell differentiation, stabilization of cytoplasmic filaments, and the chaperone activity of  $\alpha$ B crystallin (60). This hypothesis was confirmed by chaperone assays comparing the effectiveness of full-length human  $\alpha$ B crystallin and synthetic  $\alpha$ B crystallin peptides in protecting against the aggregation of FGF and VEGF. In addition, previous studies found that  $\alpha$ B crystallin inhibits the DTT and heat-induced aggregation of insulin (65–68). The results demonstrated that specific  $\alpha$ B crystallin interactive peptides were capable of protecting key regulatory proteins from unfolding and aggregation. The direct functional demonstration of  $\alpha$ B crystallin sequences provides support for the hypothesis that the chaperone function of  $\alpha$ B crystallin is not limited to stress conditions and has an important function in regulating normal cellular growth and development.

Antibodies, growth factors, enzymes, and receptors have very high substrate specificities and affinities consistent with their functional role. In contrast, sHSPs make up a class of proteins whose cytoprotective functions involve a range of substrates and cellular pathways. Interactions of sHSP with unfolding or misfolding proteins are selective and not specific. The dynamic functional mechanism of sHSP

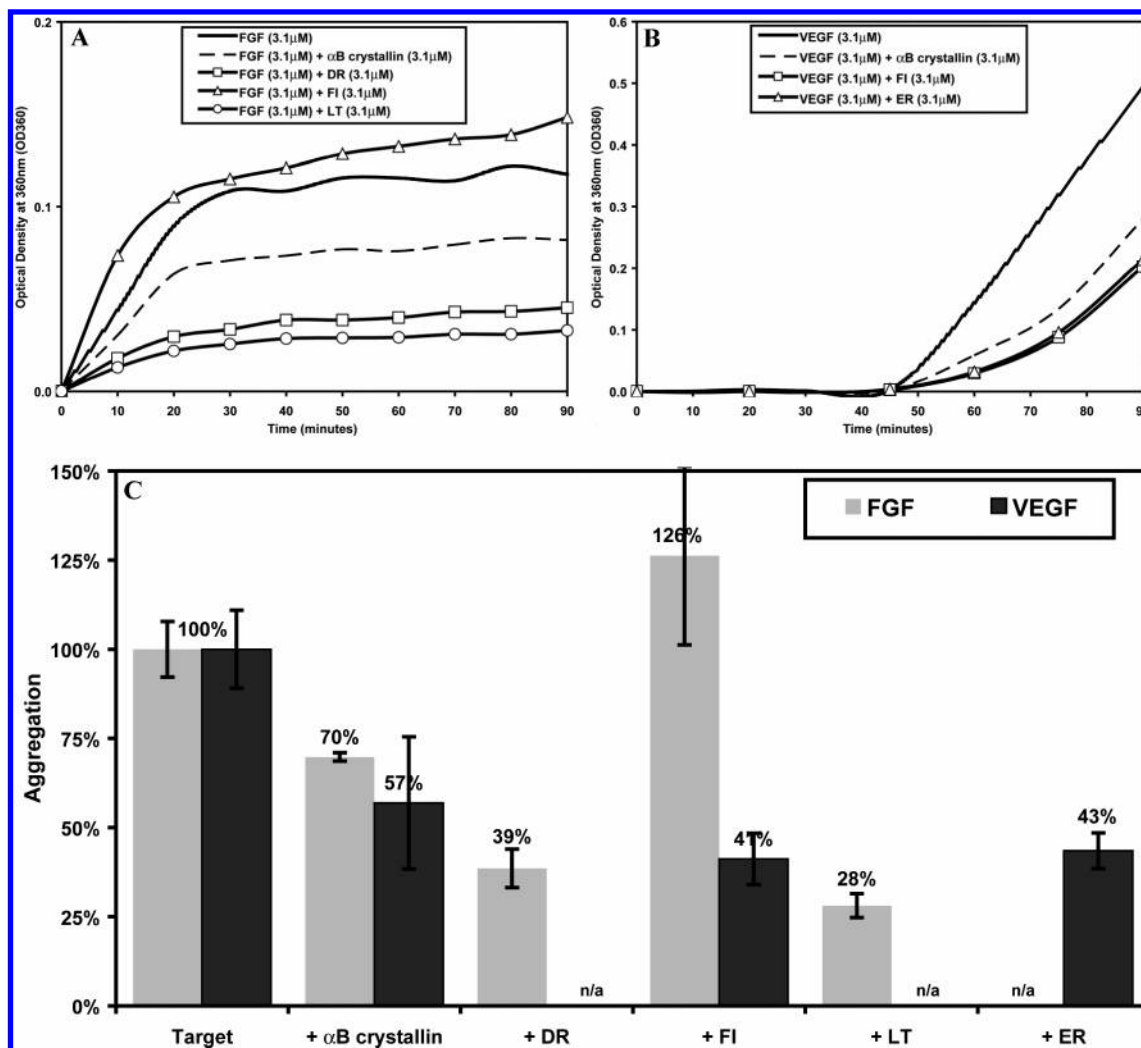


FIGURE 4: Effect of full-length wt human  $\alpha$ B crystallin and four synthetic  $\alpha$ B crystallin peptides on the aggregation of FGF-2 and VEGF. The thermal aggregation of FGF-2 at 45 °C (A) and the DTT-induced aggregation of VEGF at 37 °C (B) were assessed spectroscopically as the optical density at 360 nm ( $OD_{360}$ ) for 90 mins. The chaperone activities of full-length wt  $\alpha$ B crystallin and the  $\alpha$ B crystallin peptides were calculated using the  $OD_{360}$  measured at the end of the assay (C). The  $OD_{360}$  of the target proteins FGF and VEGF at the end of 90 mins was set to 100% aggregation. Wt  $\alpha$ B crystallin decreased FGF and VEGF aggregation by 30% and 43% respectively. The DR (DRFSVNLVDVKHFS) peptide decreased FGF aggregation by 61%. The FI (FISREFHR) increased FGF aggregation by 26%, but decreased VEGF aggregation by 59%. The LT (LTITSSLSDGV) peptide decreased FGF aggregation by 72% which was the strongest protective effect observed for the synthetic peptides. The ER (ERTIPITRE) peptide decreased VEGF aggregation by 57%. Synthetic peptides of the interactive domains of human  $\alpha$ B crystallin were effective inhibitors of aggregation.

interaction appears to be mediated by the coordination of multiple interactive sequences on the surface of assembled sHSP complexes and individual sHSP subunits (69).

Sequences involved in mediating the  $\alpha$ B crystallin–FGF interaction overlapped with previously identified  $\alpha$ B crystallin chaperone sequences (Figure 5), which was consistent with a previous report in which  $\alpha$ B crystallin was shown to promote the refolding of partially unfolded FGF at 25 °C (12). FGF is labile and structurally unstable at physiological temperatures, and the identification of FGF chaperone sequences in  $\alpha$ B crystallin suggests a biological role for the chaperone activity of  $\alpha$ B crystallin in FGF signaling (70–72). This hypothesis was supported by chaperone assays in which full-length wt  $\alpha$ B crystallin inhibited the thermal aggregation of FGF. The overlap between interactive sequences in  $\alpha$ B crystallin for VEGF and for chaperone activity was consistent with the upregulation of both VEGF and  $\alpha$ B crystallin in response to stress following myocardial infarction (56, 73, 74). The identification of chaperone sequences that mediate interactions between  $\alpha$ B crystallin and VEGF

suggests that in addition to protecting cardiac cytoskeletal proteins from unfolding and aggregation,  $\alpha$ B crystallin has a protective role in VEGF signaling during myocardial infarction (27–30, 32, 36, 56, 75–77). This hypothesis was supported by chaperone assays in which full-length  $\alpha$ B crystallin and two synthetic  $\alpha$ B crystallin chaperone sequences inhibited the aggregation of VEGF under reducing conditions. The  $\alpha$ B crystallin peptides that protect FGF and VEGF against unfolding and aggregation have the potential for use as FGF and VEGF stabilizers in therapeutic formulations for the treatment of advanced coronary artery disease (CAD) (78, 79).

Like the FGF interactive sequences in  $\alpha$ B crystallin, all four  $\alpha$ B crystallin sequences that interacted with NGF- $\beta$  overlapped with previously identified  $\alpha$ B crystallin chaperone sequences, suggesting that  $\alpha$ B crystallin may chaperone NGF- $\beta$  in vivo. These results are consistent with the role of NGF- $\beta$  in neuronal signaling and the close association of  $\alpha$ B crystallin with microtubules and microtubule-associated proteins (40, 41, 58, 80). The identification of chaperone



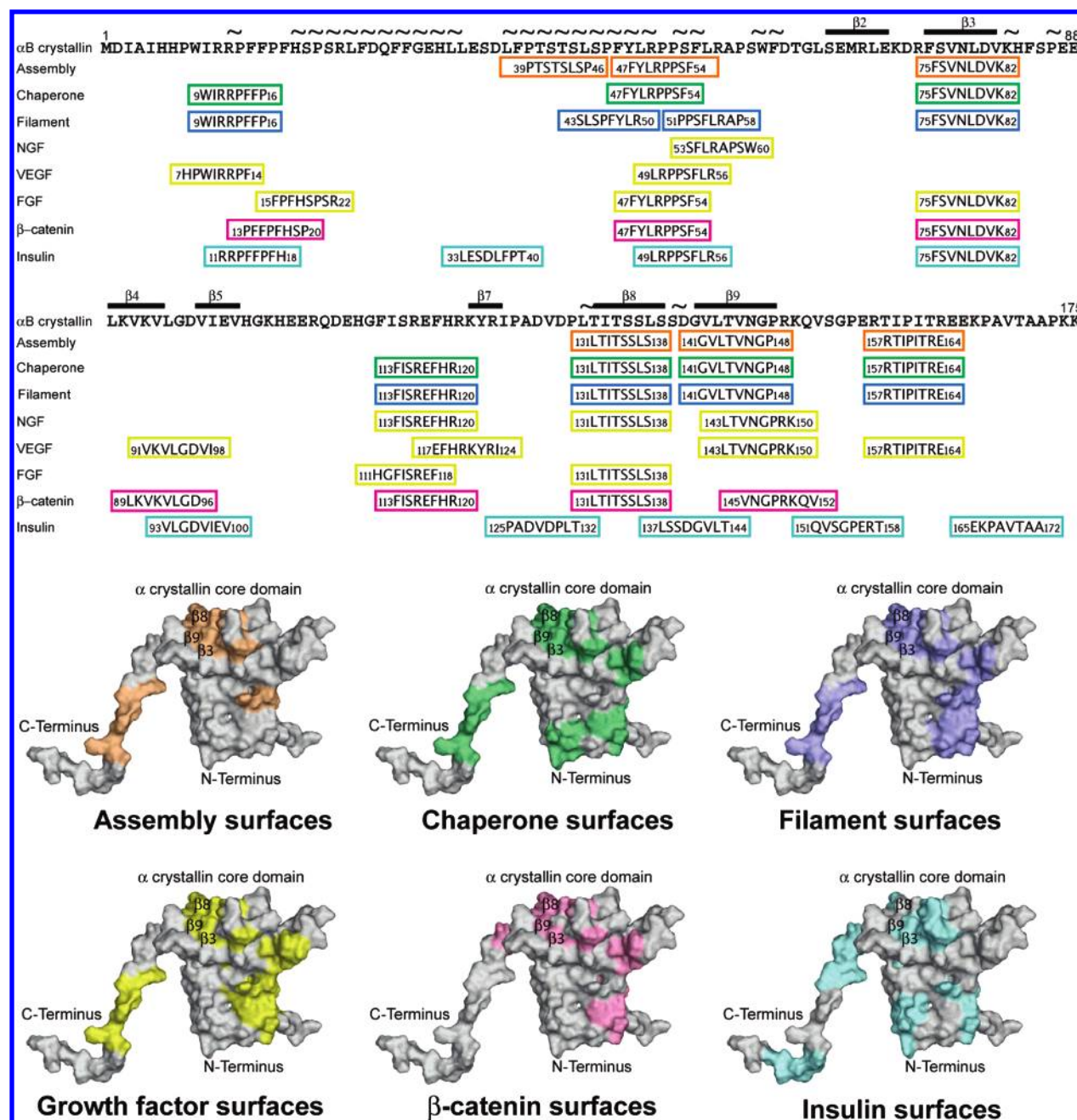


FIGURE 5: Comparison of the  $\alpha$ B crystallin interactive sequences and surfaces for subunit–subunit interactions, chaperone activity, filament interactions, growth factor interactions,  $\beta$ -catenin interactions, and insulin interactions. The secondary structure of human  $\alpha$ B crystallin is shown above its primary sequence (~ represents helix and – represents  $\beta$  strand). The interactive sequences for subunit assembly (orange), chaperone activity (green), filament interactions (dark blue), growth factor interactions (NGF- $\beta$ , VEGF, and FGF-2) (yellow), interactions with  $\beta$ -catenin (pink), and interactions with insulin (light blue) are enclosed in boxes below the primary sequence of  $\alpha$ B crystallin (top). Sequences containing  $\beta$  strands  $\beta$ 3,  $\beta$ 8, and  $\beta$ 9 as well as helical sequences in the N-terminal domain had the strongest interactions with most ligands. The interactive sequences were mapped to the surface of a three-dimensional homology model for human  $\alpha$ B crystallin, and the  $\beta$ 3– $\beta$ 8– $\beta$ 9 surface appears to be a common surface that mediates interactions with multiple proteins.

sequences for NGF- $\beta$  on the surface of  $\alpha$ B crystallin, the archetype of sHSPs, suggests that the chaperone activity of  $\alpha$ B crystallin and other sHSPs may selectively protect key growth factors and signaling molecules that are important for normal cellular processes post-stress.  $\alpha$ B crystallin colocalizes with  $\beta$ -catenin in actin networks, and like  $\beta$ -catenin,  $\alpha$ B crystallin migrates into the nucleus under conditions of cell stress in culture (34, 35, 50, 81–83). The identification of chaperone sequences in  $\alpha$ B crystallin that mediate interactions with  $\beta$ -catenin is consistent with the role of  $\alpha$ B crystallin in stabilization of cytoskeletal networks (13, 60, 61). By protecting  $\beta$ -catenin during cellular stress,  $\alpha$ B

crystallin may inhibit  $\beta$ -catenin degradation and facilitate  $\beta$ -catenin signaling through the Wnt pathway, which regulates cell proliferation and differentiation (84, 85). This hypothesis is consistent with the role of  $\alpha$ B crystallin as an anti-apoptotic and oncogenic protein (86, 87).

This is the first report of specific sequences in the sHSP and molecular chaperone,  $\alpha$ B crystallin, that interact with FGF-2, NGF- $\beta$ , VEGF, insulin, and  $\beta$ -catenin. Synthetic peptides based on the interactive sequences of  $\alpha$ B crystallin were observed to protect against the aggregation of FGF-2 and VEGF in vitro. Taken together, the results suggest the potential importance of sHSPs and molecular chaperones in



the regulation of key components of signaling pathways and cell differentiation under stress and nonstress conditions. A potential role for  $\alpha$ B crystallin in regulation of proliferation, differentiation, and structural stabilization during normal development as well as in response to stress associated with myocardial and neurodegenerative disease would be an important advance in understanding the normal function of sHSPs.

## REFERENCES

- Horwitz, J. (2003)  $\alpha$ -Crystallin, *Exp. Eye Res.* 76, 145–153.
- Haslbeck, M. (2002) sHSPs and their role in the chaperone network, *Cell. Mol. Life Sci.* 59, 1649–1657.
- Narberhaus, F. (2002)  $\alpha$ -Crystallin-type heat shock proteins: Socializing minichaperones in the context of a multichaperone network, *Microbiol. Mol. Biol. Rev.* 66, 64–93.
- van Montfort, R. L., Basha, E., Friedrich, K. L., Slingsby, C., and Vierling, E. (2001) Crystal structure and assembly of a eukaryotic small heat shock protein, *Nat. Struct. Biol.* 8, 1025–1030.
- Kim, K. K., Kim, R., and Kim, S. H. (1998) Crystal structure of a small heat-shock protein, *Nature* 394, 595–599.
- Haslbeck, M., Franzmann, T., Weinfurter, D., and Buchner, J. (2005) Some like it hot: The structure and function of small heat-shock proteins, *Nat. Struct. Mol. Biol.* 12, 842–846.
- Sun, Y., and MacRae, T. H. (2005) Small heat shock proteins: Molecular structure and chaperone function, *Cell. Mol. Life Sci.* 62, 2460–2476.
- Wisniewski, T., and Goldman, J. E. (1998)  $\alpha$ B-Crystallin is associated with intermediate filaments in astrocytoma cells, *Neurochem. Res.* 23, 385–392.
- Djabali, K., de Nechaud, B., Landon, F., and Portier, M. M. (1997)  $\alpha$ B-Crystallin interacts with intermediate filaments in response to stress, *J. Cell Sci.* 110 (Part 21), 2759–2769.
- Bennardini, F., Wrzosek, A., and Chiesi, M. (1992)  $\alpha$ B-Crystallin in cardiac tissue. Association with actin and desmin filaments, *Circ. Res.* 71, 288–294.
- Basha, E., Lee, G. J., Breci, L. A., Hausrath, A. C., Buan, N. R., Giese, K. C., and Vierling, E. (2004) The identity of proteins associated with a small heat shock protein during heat stress in vivo indicates that these chaperones protect a wide range of cellular functions, *J. Biol. Chem.* 279, 7566–7575.
- Edwards, K. L., Kuelto, L. A., Fisher, M. T., and Middaugh, C. R. (2001) Complex effects of molecular chaperones on the aggregation and refolding of fibroblast growth factor-1, *Arch. Biochem. Biophys.* 393, 14–21.
- Mounier, N., and Arrigo, A. P. (2002) Actin cytoskeleton and small heat shock proteins: How do they interact? *Cell Stress Chaperones* 7, 167–176.
- Head, M. W., Hurwitz, L., Kegel, K., and Goldman, J. E. (2000)  $\alpha$ B-Crystallin regulates intermediate filament organization in situ, *NeuroReport* 11, 361–365.
- Perng, M. D., Cairns, L., van den, I. P., Prescott, A., Hutcheson, A. M., and Quinlan, R. A. (1999) Intermediate filament interactions can be altered by HSP27 and  $\alpha$ B-crystallin, *J. Cell Sci.* 112 (Part 13), 2099–2112.
- Parcellier, A., Schmitt, E., Brunet, M., Hammann, A., Solary, E., and Garrido, C. (2005) Small Heat Shock Proteins HSP27 and  $\alpha$ B-Crystallin: Cytoprotective and Oncogenic Functions, *Antioxid. Redox Signaling* 7, 404–413.
- Quinlan, R. (2002) Cytoskeletal competence requires protein chaperones, *Prog. Mol. Subcell. Biol.* 28, 219–233.
- Djabali, K., Piron, G., de Nechaud, B., and Portier, M. M. (1999)  $\alpha$ B-Crystallin interacts with cytoplasmic intermediate filament bundles during mitosis, *Exp. Cell Res.* 253, 649–662.
- Muchowski, P. J., Valdez, M. M., and Clark, J. I. (1999)  $\alpha$ B-Crystallin selectively targets intermediate filament proteins during thermal stress, *Invest. Ophthalmol. Visual Sci.* 40, 951–958.
- Liang, P., and MacRae, T. H. (1997) Molecular chaperones and the cytoskeleton, *J. Cell Sci.* 110 (Part 13), 1431–1440.
- Prescott, A. R., Sandilands, A., Hutcheson, A. M., Carter, J. M., and Quinlan, R. A. (1996) The intermediate filament cytoskeleton of the lens: An ever changing network through development and differentiation. A minireview, *Ophthalmic Res.* 28 (Suppl. 1), 58–61.
- Gopalakrishnan, S., Boyle, D., and Takemoto, L. (1993) Association of actin with  $\alpha$  crystallins, *Trans. Kans. Acad. Sci.* 96, 7–12.
- Tomokane, N., Iwaki, T., Tateishi, J., Iwaki, A., and Goldman, J. E. (1991) Rosenthal fibers share epitopes with  $\alpha$ B-crystallin, glial fibrillary acidic protein, and ubiquitin, but not with vimentin. Immunoelectron microscopy with colloidal gold, *Am. J. Pathol.* 138, 875–885.
- Lieska, N., Chen, J., Maisel, H., and Romero-Herrera, A. E. (1980) Subunit characterization of lens intermediate filaments, *Biochim. Biophys. Acta* 626, 136–153.
- Launay, N., Goudeau, B., Kato, K., Vicart, P., and Lilienbaum, A. (2006) Cell signaling pathways to  $\alpha$ B-crystallin following stresses of the cytoskeleton, *Exp. Cell Res.* (in press).
- Maglara, A. A., Vasilaki, A., Jackson, M. J., and McArdle, A. (2003) Damage to developing mouse skeletal muscle myotubes in culture: Protective effect of heat shock proteins, *J. Physiol.* 548, 837–846.
- Morrison, L. E., Whittaker, R. J., Klepper, R. E., Wawrousek, E. F., and Glembocki, C. C. (2004) Roles for  $\alpha$ B-crystallin and HSPB2 in protecting the myocardium from ischemia-reperfusion-induced damage in a KO mouse model, *Am. J. Physiol.* 286, H847–H855.
- Golenhofen, N., Ness, W., Wawrousek, E. F., and Drenckhahn, D. (2002) Expression and induction of the stress protein  $\alpha$ B-crystallin in vascular endothelial cells, *Histochem. Cell Biol.* 117, 203–209.
- Golenhofen, N., Htun, P., Ness, W., Koob, R., Schaper, W., and Drenckhahn, D. (1999) Binding of the stress protein  $\alpha$ B-crystallin to cardiac myofibrils correlates with the degree of myocardial damage during ischemia/reperfusion in vivo, *J. Mol. Cell. Cardiol.* 31, 569–580.
- Dillmann, W. H. (1999) Heat shock proteins and protection against ischemic injury, *Infect. Dis. Obstet. Gynecol.* 7, 55–57.
- Civil, A., van Genesen, S. T., Klok, E. J., and Lubsen, N. H. (2000) Insulin and IGF-I affect the protein composition of the lens fibre cell with possible consequences for cataract, *Exp. Eye Res.* 70, 785–794.
- Xiao, X., and Benjamin, I. J. (1999) Stress-response proteins in cardiovascular disease, *Am. J. Hum. Genet.* 64, 685–690.
- Raman, B., Ramakrishna, T., and Rao, C. M. (1995) Temperature dependent chaperone-like activity of  $\alpha$ -crystallin, *FEBS Lett.* 365, 133–136.
- Bagchi, M., Katar, M., Lewis, J., and Maisel, H. (2002) Associated proteins of lens adherens junction, *J. Cell. Biochem.* 86, 700–703.
- Gusev, N. B., Bogatcheva, N. V., and Marston, S. B. (2002) Structure and properties of small heat shock proteins (sHsp) and their interaction with cytoskeleton proteins, *Biochemistry (Moscow)* 67, 511–519.
- Sun, Y., and Macrae, T. H. (2005) The small heat shock proteins and their role in human disease, *FEBS Lett.* 272, 2613–2627.
- Vinader, L. M., van Genesen, S. T., de Jong, W. W., and Lubsen, N. H. (2003) Influence of hormones and growth factors on lens protein composition: The effect of dexamethasone and PDGF-AA, *Mol. Vision* 9, 723–729.
- Nakata, K., Crabb, J. W., and Hollyfield, J. G. (2005) Crystallin distribution in Bruch's membrane-choroid complex from AMD and age-matched donor eyes, *Exp. Eye Res.* 80, 821–826.
- Crabb, J. W., Miyagi, M., Gu, X., Shadrach, K., West, K. A., Sakaguchi, H., Kamei, M., Hasan, A., Yan, L., Rayborn, M. E., Salomon, R. G., and Hollyfield, J. G. (2002) Drusen proteome analysis: An approach to the etiology of age-related macular degeneration, *Proc. Natl. Acad. Sci. U.S.A.* 99, 14682–14687.
- Wilhelmus, M. M., Otte-Holler, I., Wesseling, P., de Waal, R. M., Boelens, W. C., and Verbeek, M. M. (2006) Specific association of small heat shock proteins with the pathological hallmarks of Alzheimer's disease brains, *Neuropathol. Appl. Neurobiol.* 32, 119–130.
- Mao, J. J., Katayama, S., Watanabe, C., Harada, Y., Noda, K., Yamamura, Y., and Nakamura, S. (2001) The relationship between  $\alpha$ B-crystallin and neurofibrillary tangles in Alzheimer's disease, *Neuropathol. Appl. Neurobiol.* 27, 180–188.
- Renkawek, K., Stege, G. J., and Bosman, G. J. (1999) Dementia, gliosis and expression of the small heat shock proteins hsp27 and  $\alpha$ B-crystallin in Parkinson's disease, *NeuroReport* 10, 2273–2276.
- Renkawek, K., Voorter, C. E., Bosman, G. J., van Workum, F. P., and de Jong, W. W. (1994) Expression of  $\alpha$ B-crystallin in Alzheimer's disease, *Acta Neuropathol.* 87, 155–160.

44. Shinohara, H., Inaguma, Y., Goto, S., Inagaki, T., and Kato, K. (1993)  $\alpha$ B crystallin and HSP28 are enhanced in the cerebral cortex of patients with Alzheimer's disease, *J. Neurol. Sci.* **119**, 203–208.
45. Pountney, D. L., Treweek, T. M., Chataway, T., Huang, Y., Chegini, F., Blumbergs, P. C., Raftery, M. J., and Gai, W. P. (2005)  $\alpha$ B-Crystallin is a major component of glial cytoplasmic inclusions in multiple system atrophy, *Neurotox. Res.* **7**, 77–85.
46. Braak, H., Del Tredici, K., Sandmann-Kiel, D., Rub, U., and Schultz, C. (2001) Nerve cells expressing heat-shock proteins in Parkinson's disease, *Acta Neuropathol.* **102**, 449–454.
47. Cobb, B. A., and Petrash, J. M. (2002) Factors influencing  $\alpha$ -crystallin association with phospholipid vesicles, *Mol. Vision* **8**, 85–93.
48. Cobb, B. A., and Petrash, J. M. (2002)  $\alpha$ -Crystallin chaperone-like activity and membrane binding in age-related cataracts, *Biochemistry* **41**, 483–490.
49. Cobb, B. A., and Petrash, J. M. (2000) Characterization of  $\alpha$ -crystallin-plasma membrane binding, *J. Biol. Chem.* **275**, 6664–6672.
50. Maddala, R., and Vasantha Rao, P. (2005)  $\alpha$ -Crystallin localizes to the leading edges of migrating lens epithelial cells, *Exp. Cell Res.* **306**, 203–215.
51. Powers, C. J., McLeskey, S. W., and Wellstein, A. (2000) Fibroblast growth factors, their receptors and signaling, *Endocr.-Relat. Cancer* **7**, 165–197.
52. Gangalum, R. K., Schibler, M. J., and Bhat, S. P. (2004) Small heat shock protein  $\alpha$ B-crystallin is part of cell cycle-dependent Golgi reorganization, *J. Biol. Chem.* **279**, 43374–43377.
53. Deretic, D., Aebersold, R. H., Morrison, H. D., and Papermaster, D. S. (1994)  $\alpha$ A- and  $\alpha$ B-crystallin in the retina. Association with the post-Golgi compartment of frog retinal photoreceptors, *J. Biol. Chem.* **269**, 16853–16861.
54. Kozawa, O., Matsuno, H., Niwa, M., Hatakeyama, D., Kato, K., and Uematsu, T. (2001)  $\alpha$ B-Crystallin, a low-molecular-weight heat shock protein, acts as a regulator of platelet function, *Cell Stress Chaperones* **6**, 21–28.
55. Stoevring, B., Vang, O., and Christiansen, M. (2005)  $\alpha$ B-Crystallin in cerebrospinal fluid of patients with multiple sclerosis, *Clin. Chim. Acta* **356**, 95–101.
56. Shu, E., Matsuno, H., Akamatsu, S., Kanno, Y., Suga, H., Nakajima, K., Ishisaki, A., Takai, S., Kato, K., Kitajima, Y., and Kozawa, O. (2005)  $\alpha$ B-Crystallin is phosphorylated during myocardial infarction: Involvement of platelet-derived growth factor-BB, *Arch. Biochem. Biophys.* **438**, 111–118.
57. Andley, U. P., Song, Z., Wawrousek, E. F., Fleming, T. P., and Bassnett, S. (2000) Differential protective activity of  $\alpha$ A- and  $\alpha$ B-crystallin in lens epithelial cells, *J. Biol. Chem.* **275**, 36823–36831.
58. Katoh-Semba, R., and Kato, K. (1994) Age-related changes in levels of the  $\beta$ -subunit of nerve growth factor in selected regions of the brain: Comparison between senescence-accelerated (SAM-P8) and senescence-resistant (SAM-R1) mice, *Neurosci. Res.* **20**, 251–256.
59. Sokal, I., Haeseleer, F., Arendt, A., Adman, E. T., Hargrave, P. A., and Palczewski, K. (1999) Identification of a guanylyl cyclase-activating protein-binding site within the catalytic domain of retinal guanylyl cyclase 1, *Biochemistry* **38**, 1387–1393.
60. Ghosh, J. G., Estrada, M. R., and Clark, J. I. (2005) Interactive Domains for Chaperone Activity in the Small Heat Shock Protein, Human  $\alpha$ B Crystallin, *Biochemistry* **44**, 14854–14869.
61. Ghosh, J. G., and Clark, J. I. (2005) Insights into the domains required for dimerization and assembly of human  $\alpha$ B crystallin, *Protein Sci.* **14**, 684–695.
62. Liu, L., Ghosh, J. G., Clark, J. I., and Jiang, S. (2006) Studies of  $\alpha$ B crystallin subunit dynamics by surface plasmon resonance, *Anal. Biochem.* **350**, 186–195.
63. Ghosh, J. G., Estrada, M. S., and Clark, J. I. (2006) The function of the  $\beta$ 3 interactive domain in the small heat shock protein and molecular chaperone, human  $\alpha$ B crystalline, *Cell Stress Chaperones* **11**, 187–197.
64. Ghosh, J. G., Estrada, M. R., and Clark, J. I. (2006) Structure-based analysis of the  $\beta$ 8 interactive sequence of human  $\alpha$ B crystallin, *Biochemistry* **45**, 9878–9886.
65. Biswas, A., Miller, A., Oya-Ito, T., Santhoshkumar, P., Bhat, M., and Nagaraj, R. H. (2006) Effect of Site-Directed Mutagenesis of Methylglyoxal-Modifiable Arginine Residues on the Structure and Chaperone Function of Human  $\alpha$ A-Crystallin, *Biochemistry* **45**, 4569–4577.
66. Bova, M. P., Yaron, O., Huang, Q., Ding, L., Haley, D. A., Stewart, P. L., and Horwitz, J. (1999) Mutation R120G in  $\alpha$ B-crystallin, which is linked to a desmin-related myopathy, results in an irregular structure and defective chaperone-like function, *Proc. Natl. Acad. Sci. U.S.A.* **96**, 6137–6142.
67. Hepburne-Scott, H. W., and Crabbe, M. J. (1999) Maintenance of chaperone-like activity despite mutations in a conserved region of murine lens  $\alpha$ B crystalline, *Mol. Vision* **5**, 15.
68. Horwitz, J., Bova, M., Huang, Q. L., Ding, L., Yaron, O., and Lowman, S. (1998) Mutation of  $\alpha$ B-crystallin: Effects on chaperone-like activity, *Int. J. Biol. Macromol.* **22**, 263–269.
69. Basha, E., Friedrich, K. L., and Vierling, E. (2006) The N-terminal arm of small heat shock proteins is important for both chaperone activity and substrate specificity, *J. Biol. Chem.* **281**, 39943–39952.
70. Kardami, E., Jiang, Z. S., Jimenez, S. K., Hirst, C. J., Sheikh, F., Zahradka, P., and Cattini, P. A. (2004) Fibroblast growth factor 2 isoforms and cardiac hypertrophy, *Cardiovasc. Res.* **63**, 458–466.
71. Copeland, R. A., Ji, H., Halfpenny, A. J., Williams, R. W., Thompson, K. C., Herber, W. K., Thomas, K. A., Bruner, M. W., Ryan, J. A., Marquis-Omer, D., et al. (1991) The structure of human acidic fibroblast growth factor and its interaction with heparin, *Arch. Biochem. Biophys.* **289**, 53–61.
72. Chavan, A. J., Haley, B. E., Volkin, D. B., Marfia, K. E., Verticelli, A. M., Bruner, M. W., Draper, J. P., Burke, C. J., and Middaugh, C. R. (1994) Interaction of nucleotides with acidic fibroblast growth factor (FGF-1), *Biochemistry* **33**, 7193–7202.
73. Maulik, N. (2004) Angiogenic signal during cardiac repair, *Mol. Cell. Biochem.* **264**, 13–23.
74. Yoshiji, H., Kuriyama, S., Hicklin, D. J., Huber, J., Yoshii, J., Ikenaka, Y., Noguchi, R., Nakatani, T., Tsujinoue, H., and Fukui, H. (2001) The vascular endothelial growth factor receptor KDR/Flk-1 is a major regulator of malignant ascites formation in the mouse hepatocellular carcinoma model, *Hepatology* **33**, 841–847.
75. Martindale, J. J., Wall, J. A., Martinez-Longoria, D. M., Aryal, P., Rockman, H. A., Guo, Y., Bolli, R., and Glembofski, C. C. (2005) Overexpression of mitogen-activated protein kinase kinase 6 in the heart improves functional recovery from ischemia in vitro and protects against myocardial infarction in vivo, *J. Biol. Chem.* **280**, 669–676.
76. Martin, J. L., Bluhm, W. F., He, H., Mestril, R., and Dillmann, W. H. (2002) Mutation of COOH-terminal lysines in overexpressed  $\alpha$ B-crystallin abrogates ischemic protection in cardiomyocytes, *Am. J. Physiol.* **283**, H85–H91.
77. Ray, P. S., Martin, J. L., Swanson, E. A., Otani, H., Dillmann, W. H., and Das, D. K. (2001) Transgene overexpression of  $\alpha$ B crystallin confers simultaneous protection against cardiomyocyte apoptosis and necrosis during myocardial ischemia and reperfusion, *FASEB J.* **15**, 393–402.
78. Sellke, F. W., Laham, R. J., Edelman, E. R., Pearlman, J. D., and Simons, M. (1998) Therapeutic angiogenesis with basic fibroblast growth factor: Technique and early results, *Ann. Thorac. Surg.* **65**, 1540–1544.
79. Losordo, D. W., Vale, P. R., Symes, J. F., Dunnington, C. H., Esakof, D. D., Maysky, M., Ashare, A. B., Lathi, K., and Isner, J. M. (1998) Gene therapy for myocardial angiogenesis: Initial clinical results with direct myocardial injection of pVEGF165 as sole therapy for myocardial ischemia, *Circulation* **98**, 2800–2804.
80. Dabir, D. V., Trojanowski, J. Q., Richter-Landsberg, C., Lee, V. M., and Forman, M. S. (2004) Expression of the small heat-shock protein  $\alpha$ B-crystallin in tauopathies with glial pathology, *Am. J. Pathol.* **164**, 155–166.
81. Bhat, S. P., Hale, I. L., Matsumoto, B., and Elghanayan, D. (1999) Ectopic expression of  $\alpha$ B-crystallin in Chinese hamster ovary cells suggests a nuclear role for this protein, *Eur. J. Cell Biol.* **78**, 143–150.
82. den Engelsman, J., Gerrits, D., de Jong, W. W., Robbins, J., Kato, K., and Boelens, W. C. (2005) Nuclear import of  $\alpha$ B-crystallin is phosphorylation-dependent and hampered by hyperphosphorylation of the myopathy-related mutant R120G, *J. Biol. Chem.* **280**, 37139–37148.
83. van Rijk, A. E., Stege, G. J., Bennink, E. J., May, A., and Bloemendal, H. (2003) Nuclear staining for the small heat shock protein  $\alpha$ B-crystallin colocalizes with splicing factor SC35, *Eur. J. Cell Biol.* **82**, 361–368.

84. Pal, R., and Khanna, A. (2006) Role of smad- and wnt-dependent pathways in embryonic cardiac development, *Stem Cells Dev.* 15, 29–39.
85. Kikuchi, A., Kishida, S., and Yamamoto, H. (2006) Regulation of Wnt signaling by protein-protein interaction and post-translational modifications, *Exp. Mol. Med.* 38, 1–10.
86. Moyano, J. V., Evans, J. R., Chen, F., Lu, M., Werner, M. E., Yehiely, F., Diaz, L. K., Turbin, D., Karaca, G., Wiley, E., Nielsen, T. O., Perou, C. M., and Cryns, V. L. (2006)  $\alpha$ B-Crystallin is a novel oncoprotein that predicts poor clinical outcome in breast cancer, *J. Clin. Invest.* 116, 261–270.
87. Gruvberger-Saal, S. K., and Parsons, R. (2006) Is the small heat shock protein  $\alpha$ B-crystallin an oncogene? *J. Clin. Invest.* 116, 30–32.

BI700149H